The distribution and transport of water in oil paintings

A numerical moisture diffusion model

Duivenvoorden, Jorien R.; Kramer, Rick P.; Hommes, Margriet H.van Eikema; Iedema, Piet D.; Hermans, Joen J.; Keune, Katrien

DOI
10.1016/j.ijheatmasstransfer.2022.123682

Publication date
2023

Document Version
Final published version

Published in
International Journal of Heat and Mass Transfer

Citation (APA)
Duivenvoorden, J. R., Kramer, R. P., Hommes, M. H. V. E., Iedema, P. D., Hermans, J. J., & Keune, K. (2023). The distribution and transport of water in oil paintings: A numerical moisture diffusion model. *International Journal of Heat and Mass Transfer*, *202*, Article 123682. https://doi.org/10.1016/j.ijheatmasstransfer.2022.123682

International Journal of Heat and Mass Transfer 202 (2023) 123682

Contents lists available at ScienceDirect

International Journal of Heat and Mass Transfer

journal homepage: www.elsevier.com/locate/hmt

The distribution and transport of water in oil paintings: A numerical moisture diffusion model

Jorien R. Duivenvoorden[a,b,*], Rick P. Kramer[c], Margriet H. van Eikema Hommes[d], Piet D. Iedema[a], Joen J. Hermans[a,b], Katrien Keune[a,b]

[a] Van 't Hoff Institute for Molecular Sciences, University of Amsterdam, Science Park 904, 1098 XH Amsterdam, the Netherlands
[b] Conservation & Science, Rijksmuseum, Ateliergebouw Rijksmuseum, Hobbemastraat 22, 1071 ZC Amsterdam, the Netherlands
[c] Department of the Built Environment, Eindhoven University of Technology, Het Kranenveld 8, 5612 AZ, Eindhoven, the Netherlands
[d] Materials Science and Engineering, Delft University of Technology, Mekelweg 2, 2628 CD, Delft, the Netherlands

ARTICLE INFO

Article history:
Received 27 May 2022
Revised 3 November 2022
Accepted 17 November 2022

Keywords:
Moisture transport
Fickian diffusion
Numerical modelling
Relative humidity
Oil painting
Preventive conservation

ABSTRACT

Oil paintings are complex, multi-layered systems that are prone to chemical degradation. While it is increasingly recognised that water plays an important role in these degradation reactions, little is known about moisture concentrations in oil paint systems and their temporal variation in response to fluctuating ambient air humidity. This knowledge is necessary to further preventive conservation, specifically to establish optimal environmental conditions to safeguard works of art for future generations. We developed a transient one-dimensional moisture transport model based on Fickian diffusion enabling the integration of experimentally recorded relative humidity data. Moisture sorption and transport data for painting materials have been reviewed from literature showing that each component of a painting has rather distinct properties. Including the properties of the individual layers enabled predicting the behaviour of a multi-layered painting system. A sensitivity study indicated that the response of a multilayer is determined by the combination of diffusion coefficients, isotherm shapes, maximum water contents, layer thicknesses, period of RH fluctuation and stacking order of the layers. Finally, the model was employed to investigate a case study of 18th-century painted wall hangings in a historic house to illustrate the insights that can be gained from this approach and the types of conservation-related questions that can be answered.

1. Introduction

Like many works of art, oil paintings are complex layered systems consisting of composite materials that are subject to change on a timescale of decades. In order to safeguard these works of art for future generations, preventive conservation efforts aim to slow down or prevent this change by optimising environmental storage and display conditions, and exercising risk mitigation. The ethical considerations within the cultural heritage context also strongly restrict the degree to which conservators can alter a work of art when attempting to undo unwanted material change. Thus, preventive conservation is considered an effective and sustainable art conservation strategy [1]. Fundamental to this approach to conservation is that we should have a thorough understanding of the mechanisms of material change in artworks and the environmental factors that influence deterioration. In recent decades, considerable progress has been made towards elucidating the mechanisms of chemical degradation in oil paintings. Many of these studies have pointed to the negative influence of water on the chemical deterioration of oil paints [2–22]. In a cultural heritage context, a painting can be exposed to water from different sources. Paintings are exposed to ambient air for multiple decades or centuries in historic buildings, on public display in museums or in storage in museum depots. Short term water exposure could occur during restoration interventions such as cleaning or consolidation treatments that involve water. Also, in a worst-case scenario, a painting can experience extreme water exposure during events like leakages or floods.

To understand the kinetics of oil paint degradation reactions involving water, a key step is to investigate the water content in a painting under varying environmental conditions. Despite the importance of this objective, complete multi-layered oil paint systems have not yet been studied in detail from the point of view of thermodynamics and transport phenomena. Hence, this study focuses on the transport and distribution of water in an oil paint-

* Corresponding author.
E-mail addresses: j.duivenvoorden@rijksmuseum.nl (J.R. Duivenvoorden), r.p.kramer@tue.nl (R.P. Kramer), m.h.vaneikemahommes@tudelft.nl (M.H.v.E. Hommes), p.d.iedema@uva.nl (P.D. Iedema), j.j.hermans@uva.nl (J.J. Hermans), k.keune@rijksmuseum.nl (K. Keune).

https://doi.org/10.1016/j.ijheatmasstransfer.2022.123682

Table 1
Overview of typical paintings' materials.

Layer	Composition	General chemical composition	References
varnish	natural resin	mixture of triterpenoids	
oil paint	drying oil	polymer network of unsaturated triacylglycerides	[23–25]
	pigment	metal salts, minerals or organic dyes	
ground layer	animal glue	collagen (helical protein chains)	[26,27]
	chalk	calcium carbonate	[28]
canvas	woven linen, pre-treated with glue sizing	cellulose fibres and collagen	[29,30]

ing stratigraphy as a result of environmental humidity fluctuations, providing a first step towards correlating chemical deterioration patterns to a painting's environmental conditions. A major challenge is the wide variability of the, often natural, paint materials involved, with compositions that are neither constant nor well-defined within or across objects. Table 1 shows some details on the function and composition of the materials considered in this paper.

The topic of moisture transport through multi-layered polymer systems has been addressed quite extensively, both experimentally and theoretically, in research fields dealing with industrial coatings and commercial paints [31–38]. In addition, computational modelling of transport processes is a well-established practice [39–43]. However, in cultural heritage research, only few studies have been dedicated to spatially resolved quantification of water concentrations inside multi-layered paint systems, usually using either Nuclear Magnetic Resonance (NMR) imaging [44] or neutron radiography [44–47]. However, these techniques tend to provide insufficient spatial resolution for measuring water concentrations in thin layers, and the techniques can be difficult to access. Although other techniques such as ^{1}High-Resolution-Magic-Angle-Spinning (HR-MAS) NMR spectroscopy, infrared (IR) spectroscopy and gravimetric analysis may provide valuable information on moisture diffusion and sorption properties of paint films, they are usually bulk techniques that do not provide spatially resolved information [3,9,48–52]. Finally, mobile unilateral NMR devices, such as the NMR Mouse, with their unique capability for *in-situ* diffusion studies have limitations in resolution, sample size and measuring depth [53,54].

Numerical modelling of moisture transport has been applied previously in the context of cultural heritage. Most studies have focused on the mechanical effects induced by moisture sorption in sensitive wooden objects [47,55,56,57]. Rachwal et al. (2012) [56] developed a two-layered model to calculate moisture diffusion through wood and gesso (rabbit skin glue with chalk). However, only very few studies have applied numerical modelling to multi-layered systems representing canvas paintings. Ferrer et al. (2022) employed moisture transport modelling to evaluate the efficacy of aluminum backplates for canvas paintings [58], while Lee et al. (2022) investigated the mechanical response of canvas paintings to dessication [59]. Oil paintings are particularly interesting objects to simulate, because the oil-based paint layer has very slow transport properties compared to the other components of the painting resulting in a complex response to fluctuating environmental conditions. The diffusion coefficient of water in an oil-based paint ($\sim 10^{-13}$ m^2/s) is markedly lower compared to other well-known polymer films such as cellulose acetate ($\sim 10^{-11}$ m^2/s), polyvinyl acetate ($\sim 10^{-11}$ m^2/s) and 6-10 nylon ($\sim 10^{-12}$ m^2/s) [60]. In fact, the diffusion coefficient of water in oil-based paints is closer to those of barrier coatings tested for the automotive industry ($\sim 10^{-13}$–10^{-12} m^2/s) [31,40].

We have developed a transient one-dimensional moisture transport model for painting stratigraphies based on moisture transport and sorption parameters collected from literature. This diffusion model is evaluated using a method-of-lines approach and it allows quantification of water concentration in all layers of an oil painting, including paint layers, preparatory layers and the canvas support. Each layer is considered as a continuous solid medium of constant thickness. Ideal diffusion has been used previously to describe water sorption in oil paint [3,49,61]. Baij et al. (2018) developed a Fickian diffusion-swelling model that forms the basis of the model presented in this paper [3]. They showed that film swelling can strongly influence overall sorption behaviour. However, as water only caused minimal expansion of linseed oil-based polymer films (less than 5%), swelling is not considered in the current model. For other layers found in an oil painting, especially those containing animal glue (which contains 12–15 wt% water at 50% relative humidity [26]), minimal swelling could be a more tenuous approximation.

In order to accurately predict moisture sorption behaviour, considering the full painting stratigraphy is essential. In this paper, we demonstrate that each layer can have a profound influence on the moisture response of the entire system. The current model requires as input two bulk properties per layer of the painting stratigraphy: a moisture sorption isotherm and a diffusion coefficient. With this input, the model can be used to make general predictions about moisture transport and distribution in multi-layered systems. Moreover, the ability to directly relate experimentally recorded relative humidity values to local moisture concentrations makes this model especially suitable for conservation applications. A particularly relevant application for the model and the insights it generates is assessing the guidelines for indoor climate in heritage institutions that are currently under discussion in the face of the energy and climate crisis [62]. A case study that considers the 18th-century painted wall hangings in the salon of the Hofkeshuis (Almelo, the Netherlands) will demonstrate the application of the model. The painted wall hangings have been the subject of previous investigations into the correlation between the indoor climate and deterioration of oil paint [63–66]. Those studies indicated that the oil paint on the south wall showed a higher degree of chemical degradation in deeper paint layers than near the surface. It was hypothesised that this observed deterioration pattern could be explained by a higher concentration of water in the lower paint layer caused by a high relative humidity behind the wall hangings. Hence, the current model is used to test whether a gradient in relative humidity between the front and the back of the wall hangings could lead to a gradient in moisture content in the paint layers.

2. Method

2.1. Thermodynamics: sorption isotherms

In this study, we consider the situation where solid films absorb water as a result of exposure to humid air. The thermodynamic equilibrium between humid air and wet film is described by moisture sorption isotherms. These isotherms are usually plotted as water concentration, also known as Equilibrium Moisture Concentration (EMC), in the material (c_{H_2O}) versus relative humidity (RH), which is equal to the ratio between partial water vapour pressure and saturated water vapour pressure, $p_{H_2O}/p^0_{H_2O}$, or the activity coefficient of water in air, a_{H_2O}. The moisture sorption capacity of a material is indicated in this paper by c_{95}, i.e. the water concen-

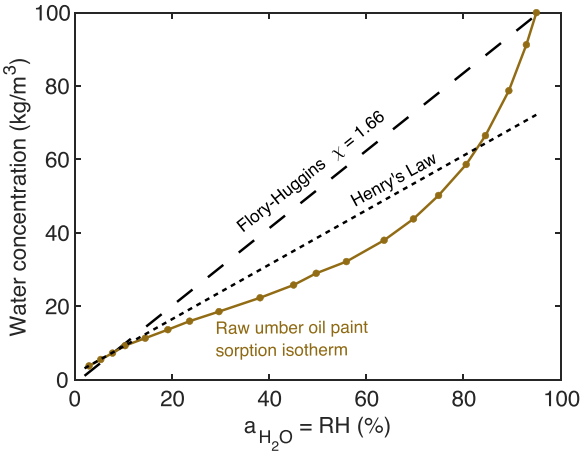

Fig. 1. Moisture sorption isotherm of raw umber oil paint [51], as water activity coefficient, a_{H_2O}, equal to RH (%), versus water concentration. For comparison, Henry's law is shown with the same slope as the sorption isotherm at $c_{H_2O} \rightarrow 0$. The isotherm also deviates strongly from the Flory-Huggins curve with $\chi = 1.66$.

tration at 95% RH. It must be noted that animal glues experience a change in material characteristics at high RH, i.e. roughly above 70% RH [26,67,68]. Therefore, the experimentally recorded sorption data of glue above 70% RH may be less reliable. Nevertheless, for the sake of consistency, the moisture sorption capacity of each material is indicated by c_{95}. A linear relation between a_{H_2O} and c_{H_2O} with the slope of the sorption isotherm at $c_{H_2O} \rightarrow 0$ represents Henry's Law [69], according to

$$p_{H_2O} = K c_{H_2O} \tag{1}$$

where K is Henry's constant. Hydrophobic polymers with a low water absorption capacity typically follow Henry's Law [40]. However, Fig. 1 shows a typical isotherm of a raw umber oil paint which deviates from this linear relation. Here, the x-axis shows the activity of water vapour in the air, and the y-axis the concentration of water in the paint. For polymer systems, Flory-Huggins theory may be more accurate, based on Flory's well-known lattice model for mixed polymer systems [70].

$$ln(a_{H_2O}) = ln\left(p_{H_2O}/p^0_{H_2O}\right) = ln(\varphi_1) + \varphi_2 + \chi(\varphi_2)^2 \tag{2}$$

Here, $\varphi_1$and φ_2 are volume fractions solvent and polymer, respectively, while χ is the interaction parameter. For the raw umber oil paint isotherm, a value for χ of 1.66 was found based on c_{95}, but the Flory-Huggins curve still deviates significantly from the measured sorption isotherm (Fig. 1). More detailed models describing sorption isotherms of various shapes are available, for instance the GAB (Guggenheim, Anderson and de Boer) model [37]. The shapes of the isotherms presented here may best be described as a Type II shape of the GAB model. For improved accuracy, in the present paper we will use experimental sorption isotherms in all calculations instead of idealised sorption models. The experimental sorption isotherms are linearly interpolated. No significant hysteresis in the isotherms of the materials considered in this paper was found in literature. For that reason, the model does not incorporate hysteresis.

2.2. Transport properties: Fickian diffusion

Our transport model is based on Fick's second law, applied to moisture transport in one dimension in the direction perpendicular to the paint surface in a massive, continuous solid, assuming a constant diffusion coefficient for each layer. Assuming ideal diffusion, we do not allow for swelling and the corresponding extra drift or convective transport equation. We assume that the values for diffusion coefficients are independent of moisture content. Fick's second law is expressed with a second-order partial differential equation (PDE):

$$\frac{\partial c}{\partial t} = D\,\frac{\partial^2 c}{\partial x^2} \tag{3}$$

Here, c is the water concentration in kg/m^3 (the subscript 'H_2O' is dropped) and D is the diffusion coefficient. Eq. 3 is solved using a discretization scheme as depicted in Fig. 2 and Eq. 4, where each layer is discretised in n slices with constant thickness h. c_n refers here to the bulk moisture concentrations in the centre of each slice n.

$$\frac{\Delta c}{\Delta t} = \frac{D\frac{c_{n+1}-c_n}{h} - D\frac{c_n-c_{n-1}}{h}}{h} \tag{4}$$

Furthermore, solving the PDE in Eq. 3 requires the formulation of proper boundary conditions. For our multi-layered systems, we assume equilibrium at the interfaces between layers and at both system-air interfaces. At the interface between a layer and air, the equilibrium concentration c_{eq} is obtained from the sorption isotherm, which sets the boundary condition at air-interface:

$$c_{eq} = f(a) = f(RH) \tag{5}$$

Here, $f(a)$ represents the sorption isotherm as a function of water activity coefficient. The water activity coefficient is equal to RH. The boundary conditions between the various layers are also inferred from the sorption isotherms. The equilibrium concentrations c^* at interface between adjacent layers 1 and 2 are stated as follows.

$$c^*_1 = f_1(a) \text{and } c^*_2 = f_2(a) \tag{6}$$

These provide the distribution coefficient as a function of activity.

$$m(a) = c^*_1/c^*_2 \tag{7}$$

The boundary conditions follow from the interface concentrations in Eqs. (4) and (6) and from the continuity condition of equal fluxes at both sides of each interface. With each layer discretised into n slices, this continuity condition reads as follows.

$$D_1\left(c^*_{1,n} - c^{bulk}_{1,n}\right) = D_2\left(c^{bulk}_{2,1} - c^*_{2,1}\right) \tag{8}$$

Note that Eq. 7 applies to the equilibrium concentrations in the slices, $c^*_{1,n}$ and $c^*_{2,1}$. The equilibirium concentrations $c^*_{1,n}$ and $c^*_{2,1}$ are solved by combining Eqs. 7 and Eq. 8.

The transport model was implemented and solved in MATLAB using a standard MATLAB ODE solver (ode15s) [71,72]. A typical script used for the calculations in this study can be found in the **SI**. Research data is available on reasonable request. The model was validated against high resolution NMR imaging data of moisture absorption and desorption in a bilayer coating system [31,40]. This bilayer coating system consisted of a hydrophobic solventborne top coat and a hydrophilic waterborne base coat. Results of the numerical model using material properties reported by the authors of the NMR study were in good accordance with the experimental sorption data. Details of this validation step can be found in the **SI**.

2.3. Parameter estimation

The aim of our parameter estimation approach was to obtain adequate estimates of the diffusion coefficients (D) and moisture sorption isotherms for each layer in an oil painting stratigraphy based on the rather limited amount of data available in literature. Three approaches for estimating these parameters were used: (i) Available information in literature was converted into data with

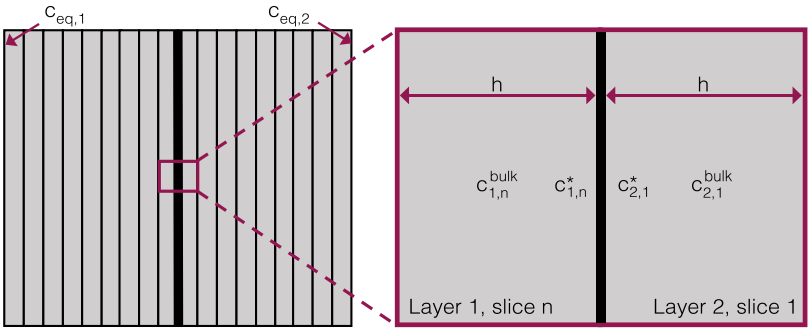

Fig. 2. Schematic representation of the bilayer system and the interface between layer 1 and 2. c_{eq} denotes the water concentration at the air interface. c^{bulk} denotes the bulk moisture concentration at the centre of each slice n, as defined in Eq. 4. c^{*} denotes the equilibrium moisture concentrations at the layer-layer interface.

Fig. 3. South wall of the salon in the Hofkeshuis, Almelo in 1981, showing painted wall hangings on either side of the mantel piece. Image: Rijksdienst voor het Cultureel Erfgoed, Amersfoort / 225.788.

suitable units for incorporation in the model; (ii) Sorption experiments from literature were simulated using the model, replicating the experimental set-up as closely as possible with respect to layer build-up, layer thickness and humidity conditions, enabling the estimatation of the diffusion coefficients and water concentrations at saturation; (iii) Properties of mixtures or composites were estimated based on the individual components of those mixtures. The parameter estimation is discussed in more detail in Section 3.1.

2.4. Case study Hofkeshuis

The case study concerns a set of wall hangings painted by Andries Warmoes in 1778 covering all four walls of a salon in a private house in Almelo (the Netherlands), known as the Hofkeshuis [63]. Executed in oil on canvas hangings stretched onto wooden battens, the paintings depict a Roman procession in imitation relief (Fig. 3). The colour palette contains only beige and brown shades to imitate stonework. It consists of chalk, black and brown earth pigments, and lead white. The painting stratigraphy is composed of two paint layers on top of a chalk-glue ground. Microscopic analysis revealed that the lead white pigment has partly reacted with free fatty acids in the oil to form slightly transparent lead soaps, disrupting the visual effect originally intended by Warmoes [63]. The outcome of a systematic study of lead soap formation in the paintings demonstrated that the degree of degradation of the lead white pigment is rather variable throughout the room and between paint layers. The researchers suggested that the variable environmental conditions in the salon have influenced the deterioration patterns [65,66]. The paintings form a rare opportunity to study the effect of the environment on paint deterioration in isolation, because the paintings have undergone relatively little restoration treatment.

The relative humidity and temperature were measured at various locations in the salon over the course of one year in 2013. A second investigation was performed focusing on temperature effects due to sunlight hitting the paintings [64]. In the current paper, we focus on the south wall of the salon, which does not receive direct sunlight. The paintings on this wall experienced chemical degradation in the form of lead white breakdown and lead soap formation deeper inside the paint stratigraphy [65].

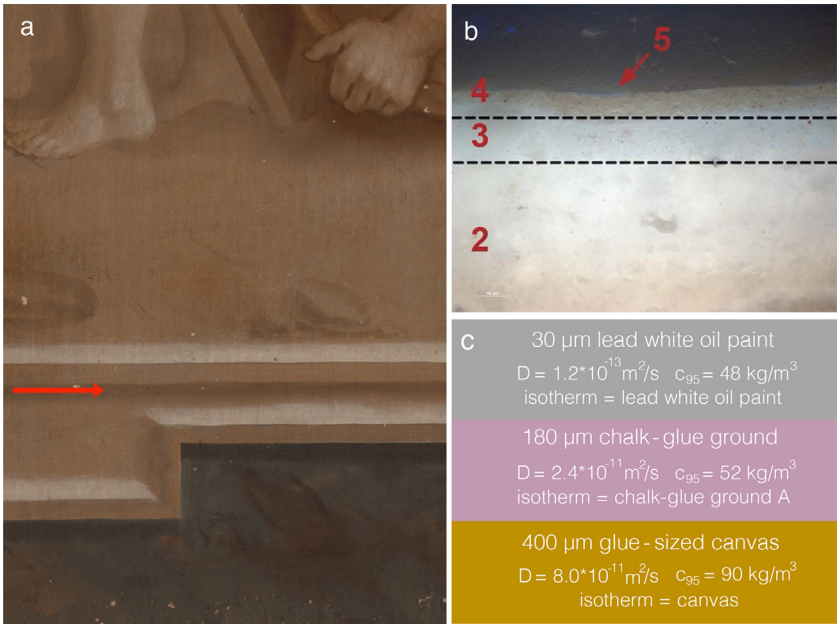

Fig. 4. a) Painted border along which samples were taken for analysis. Image by Keune et al. (2016) [65]. **b)** Light microscopy image of cross-section of a sample of the painted wall hangings. Layer 2 is the chalk-glue ground and layers 3 and 4 the lead white based paint. Layer 5 is a very thin (1–2 μm) varnish layer. Image by [65]. **c)** Schematic image (not to scale) of the reconstructed stratigraphy with the values chosen for the model parameters. The number of slices per layer was chosen to achieve constant slice thickness ($h = 1$ μm).

A current hypothesis is that a raised relative humidity behind the wall hangings has led to a higher concentration of water in the lower paint layer and could have contributed to a higher degree of lead white degradation in that layer. We used the moisture transport model to investigate whether the relatively small difference in RH between the sides of the canvas leads to such higher water concentrations in support of this hypothesis. To that end, a simplified stratigraphy of the painted wall hangings was constructed in the model. The paintings are executed in a lead white mixture on a chalk-glue ground and a glue-sized canvas. These findings are based on cross-section analysis of microscopic samples taken from the painted border (Fig. 4a) [63,65]. The paint layer consists of two applications of similar paint (Fig. 4b): layer 3 (approximate thickness 20 μm) and 4 (approximate thickness 10 μm). They are represented as one layer with the same properties in the model (Fig. 4c). Moreover, a varnish layer is present on the paintings, which was probably applied in 1957. The varnish layer is omitted from the simulations, because it is very thin (1–2 μm), diminishing its effect on overall moisture transport. The values for the model parameters are chosen based on the findings presented in Section 3.1 and are summarised in Fig. 4c.

2.5. Environmental monitoring and data preparation

The environmental data used for the analysis was recorded between 31 October 2012 and 7 October 2013 in the salon of the Hofkeshuis. Relative air humidity (RH) and air temperature (T_a) were recorded close to the west wall at 1.0 m above floor level. The relative humidity and surface temperature (T_s) behind the painted wall hangings were recorded on the south wall, through a pre-existing hole in the wall hangings. The interval between each measurement was 10 minutes. The missing data points in the data set (1% of the total data set) were replaced with the last measured value. The absolute humidity (AH) in kg/m^3 was calculated using RH and T, according to the formula described in a recent paper by He et al. (2021) [73]. Table 2 shows the specifications of the sensors that were used to measure relative humidity and temperature.

Table 2
Specification of instruments that were used for the indoor climate measurements.

Variable	Range	Accuracy	Sensor
Temperature [°C]	-80 150	±0.1	NTC type DC95
Relative Humidity [%]	0 100	±3	Humitter® 50YX

3. Results

3.1. Parameter estimation

3.1.1. Moisture sorption isotherms

Fig. 5 shows moisture sorption isotherms of the materials relevant to the current study [47,51,61,67]. In the literature sources, the isotherms were reported as sample mass gain in percentages. Using common values for the density and typical critical pigment volume concentration (CPVC) or reported mixture ratios, the percentage mass gain was converted to water concentration in kg/m^3.

Fig. 5a shows the isotherms of relevant materials with a high sorption capacity. Multiple isotherms of animal glues were found in literature and are in good agreement [47,51,56,67]. Traditionally, animal glue had many uses in painting practice, for instance for the preparation of canvas (sizing) or as a binding medium for chalk-glue ground layers.

Materials with a c_{95} in the mid-range are shown in Fig. 5b. The curve representing canvas is the result of combining different sources of information. The isotherm shown here corresponds to a medium coarse plain linen weave canvas, recorded by Hendrickx and co-workers (2016) [51]. Its maximum mass gain lies around 20%, which is in good agreement with an NMR Mouse measurement of unsized canvas at saturation [44]. However, some issues were encountered when converting mass gain to water concentration, as the density (kg/m^3) of the plain linen weave canvas was unknown. Using an estimate of the density of the canvas by combining the surface density (372 g/m^2) and its thickness (±500 μm) resulted in a c_{95} of 142 kg/m^3. This value seems unreasonably high when compared to the results of a neutron radiography sorption

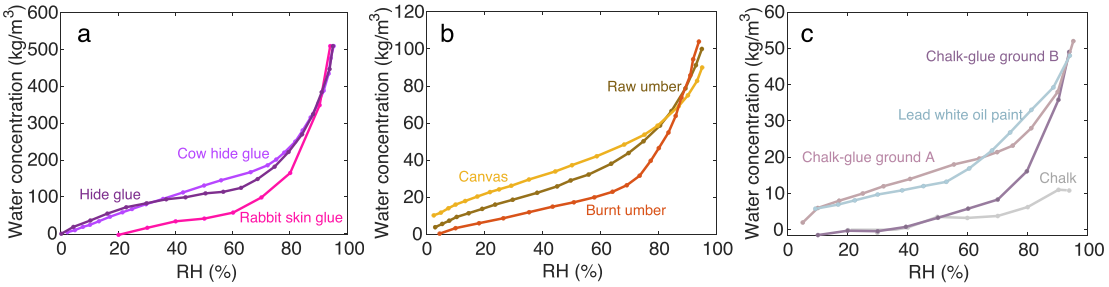

Fig. 5. Moisture sorption isotherms of relevant material adapted from literature. Rabbit skin glue, chalk-glue ground B, chalk (Champagne): [67]. Cow hide glue, canvas, raw umber, chalk-glue ground A: [51]. Hide glue: [47]. Burnt umber, lead white oil paint: [61].

test of sized canvas [44]. In that experiment, sized canvas reached 0.08 cc/cc volumetric moisture content (80 kg/m^3) after 3 hours at 90% RH. For the purposes of this paper, using the isotherm shape of canvas, this reported water concentration at 90% RH was converted into a c_{95} of 90 kg/m^3, as shown in Fig. 5b.

Oil paints can exhibit quite a wide range in moisture sorption capacity, as became apparent from MacBeth's study (1988) of 11 samples of oil paints containing different pigments [61]. In this study, the burnt umber oil paint was among the paints with the highest moisture sorption capacity. It is important to realise that earth pigments such as umbers and ochres may vary considerably in their moisture sorption capacity [67], likely due to differences in clay content. In Fig. 5b, sorption isotherms of umber paints from two different literature sources are presented [61,67]. Lead white oil paint, on the other hand, is amongst the paints with lowest sorption capacity [3,49,61]. The c_{95} of lead white oil paint is approximately a factor 2 smaller than that of umber oil paint (Fig. 5c).

In this study, chalk has the lowest moisture sorption capacity of all considered materials [51,56,67]. Although a chalk-glue ground contains animal glue, this material still falls in the low c_{95} category. The moisture sorption capacity depends mostly on the amount of glue present in the mixture. Chalk-glue grounds from two different literature sources with comparable chalk:glue ratios (92% and 83% w/w) are shown in Fig. 5c [51,67]. Although their c_{95} is similar, the isotherm shapes differ slightly. The isotherm of gesso (another type of chalk-glue mixture) from a third literature source agrees well with the data in Fig. 5c [56].

3.1.2. Diffusion coefficients

Data on moisture transport properties of artists' materials is scarce in literature. Fig. 6 summarises our findings. The diffusion coefficients of water in a few oil paints were available in literature [3,47,49]. Although they contain different pigments, the diffusion coefficients are all in the order of 10^{-13} m^2/s. In addition, diffusion coefficients reported for polymerised lead ionomer model systems agree at approximately $6{*}10^{-13}$ m^2/s [3]. In contrast to oil paints, hide glue has a typical diffusion coefficient three orders of magnitude higher around 10^{-10} m^2/s [47].

The diffusion coefficients for sized canvas and chalk-glue ground were found by modelling experimental moisture sorption data reported by Hendrickx and co-workers (2017) [44]. The experiment in question is a neutron imaging experiment measuring the water absorption of a three-layered model system: umber oil paint, chalk-glue ground and sized canvas. From dry conditions, the RH was raised to 90% and the water absorption in the model system was measured for 3.5 hours using a neutron radiography set-up. The three layers were replicated in the model, using the isotherms for raw umber oil paint, chalk-glue ground and sized canvas as reported by Hendrickx et al. (2016) [51] (Fig. 7a). The RH conditions

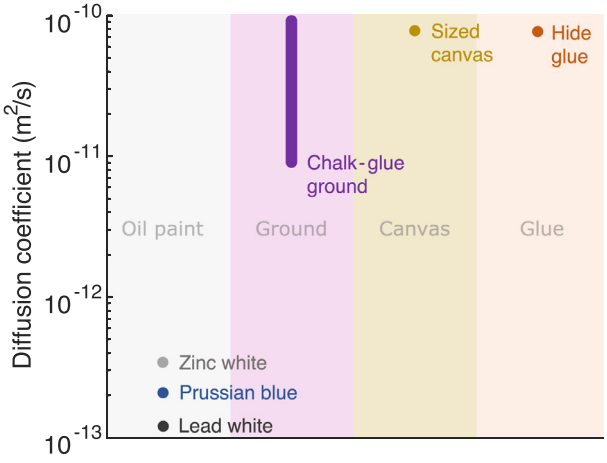

Fig. 6. Overview of diffusion coefficients of relevant materials adapted from literature. Zinc white: [3]. Prussian blue and lead white: [49]. Hide glue: [47]. Chalk-glue ground and sized canvas are based on [44].

were increased from 1% to 90%. The c_{95} for umber oil paint was set to 100 kg/m^3 based on Hendrickx et al. (2016) [51]. For the chalk-glue ground and sized canvas, the average of the final 15 experimental data points was taken (represented by the solid data points in Fig. 7b) and converted using the isotherm to c_{95}: 46 kg/m^3 for the chalk-glue ground and 90 kg/m^3 for sized canvas.

Fig. 7b shows the results of the simulations. The best combination of diffusion coefficients (D) for the ground and canvas was found by systematically trialing sets of diffusion coefficients and evaluating them according to a least-squares fit criterion. The three-layered system appeared to be much more sensitive to changes in D_{canvas} than in D_{ground}, because in this system the canvas is rate-limiting. Therefore, for the chalk-glue ground merely the lower limit for the value of D_{ground} (10^{-11} m^2/s) could be established. Any value above this limit did not influence the concentration profile as shown in Fig. 7b. For glue-sized canvas, it was possible to further narrow down the value for the diffusion coefficient ($8{*}10^{-11}$ m^2/s).

To further specify the value for D_{ground}, the assumption can be made that the diffusion rate of water in the ground layer is mostly determined by the presence of glue that acts as the binding medium. Therefore, we may assume that $D_{\text{ground}} \approx xD_{\text{hideglue}}$, where x is the volume fraction of glue in the chalk-glue mixture. For a 1:1 w/w chalk-glue ground [51], $x = 0.3$. Finally, it must be noted that the rate of desorption in the experimental data (starting at 220 minutes) is nearly instantaneous, much higher than the rate of absorption. The reason for this very rapid desorption is unclear to us, and therefore we did not simulate this part of the experiment.

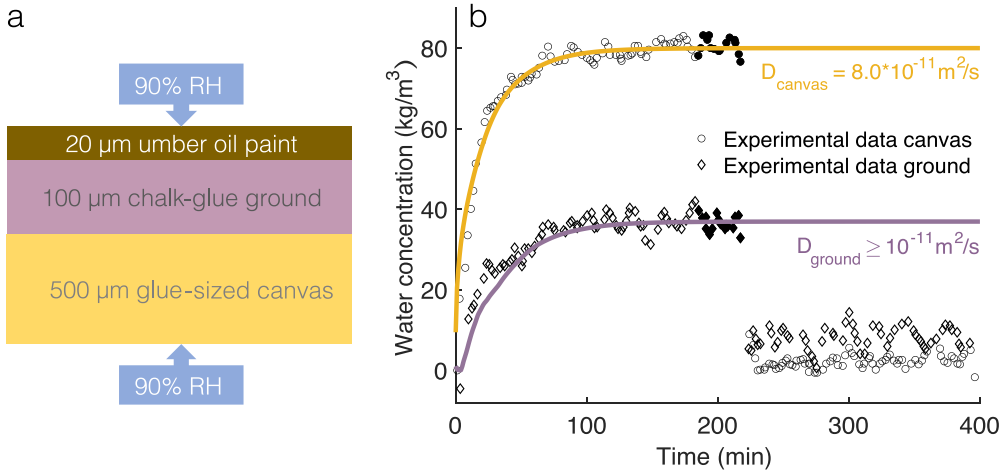

Fig. 7. **a)** Schematic representation of the layers of the sample as replicated in the model. **b)** Experimental data points adapted from [44]. The coloured curves corresponding the results of the simulation. The solid data points were used to calculate the c_{95} of the chalk-glue ground and sized canvas.

A second study that discusses experimental data on the diffusion of water in canvas is by Gregers-Høegh and co-workers (2019) [50]. They reported the time needed for their samples to reach 75% (t_{75}) of the equilibrium mass change when the RH was increased from 42% to 69%. The t_{75} of their untreated canvas was in the range of 14 to 30 minutes, while the t_{75} of wax-resin impregnated canvas samples was around 103 hours. To see how our calculated diffusion coefficient compared to their results, the t_{75} of a layer of canvas ($D = 8{*}10^{-11}$ m^2/s, $c_{95} = 90$ kg/m^3) was calculated. The thickness of the samples from Gregers-Høegh et al. is unknown. Based on the reported thickness of the individual canvas treads, we estimate a thickness between 600–800 μm. This estimate results in a t_{75} ranging between 9 and 15 minutes. Since these t_{75} values are in the same order of magnitude as those reported by Gregers-Høegh et al., this result gives some additional confidence for our estimate of the diffusion coefficient for canvas.

3.2. Sensitivity study

The discussion in Section 3.1 demonstrates that there remains some uncertainty in the values for the input parameters of the moisture transport model. This uncertainty is a consequence of the relatively small number of suitable experimental studies on moisture transport, ambiguity in the composition of samples or measurement conditions in those experimental studies, and a potential mismatch in properties between the reconstructions and model systems in experimental studies and real heritage materials. However, it is important to note that uncertainty in material properties is an unavoidable reality when dealing with aged cultural heritage objects, due to the large inherent variations in material composition and object history. Therefore, to support our parameter estimation it is essential to explore the sensitivity of the transport model to variation in parameter values. For each layer in the painting stratigraphy, the model parameters are the layer thickness, the diffusion coefficient (D) and the moisture sorption isotherm. The latter can be divided into two components: the shape of the isotherm and the water concentration at 95% RH (c_{95}) as a scaling factor. Each of the four parameters was varied for a monolayer test system with a thickness 500 μm, which was subjected to a sine-wave shaped RH fluctuation (30–70% with a 24h period, with 50% as initial condition). In addition, we varied the period of the RH oscillation as a fifth parameter.

Fig. 8a shows the influence of the isotherm shape of the three materials with mid-range moisture sorption capacity (Fig. 5b). The main difference between the time profiles in is the average water concentration around which the profile oscillates, while the shape of the concentration profiles remains comparable. Both observations can be explained by considering the isotherms in Fig. 5b. At the same RH, canvas has a higher moisture sorption capacity than both raw umber and burnt umber, but the shape of all three isotherms is almost linear between 30 and 70% RH. Fig. 8b shows that, as expected, c_{95} effectively scales the concentration profiles, leading to an increase both in the average water concentration and the amplitude of the fluctuation.

The effects of changing the diffusion coefficient are shown in Fig. 8c. The first step between 10^{-10} and 10^{-11} m^2/s does not cause a large change in the concentration profile. However, decreasing the value of D one more order of magnitude to 10^{-12} m^2/s leads to a dampened response. The amplitude of this concentration profile is lower, and the response is delayed with respect to the peak in external RH. Lowering the value of D to the range of a typical oil paint (10^{-13} m^2/s) results in an almost entirely dampened concentration profile. Under these conditions, water does not penetrate this system fast enough to the centre of the layer to keep up with the external changes in humidity. Fig. 8c does show that the average of the brown curve ($D = 10^{-13}$ m^2/s) is increasing slightly over time. Running a longer simulation, it was observed that the average of this curve stabilises at a water concentration that corresponds to approximately 52% RH. This increase from 50 to 52% RH seems to be an effect of the shape of the raw umber isotherm.

The same curve, corresponding to a diffusion coefficient in the oil paint range ($D = 10^{-13}$ m^2/s), is shown in Fig. 8d on a much longer timescale. This D was kept constant, while the period of the RH sinusoidal fluctuation was increased. It is clear that the response of the monolayer with slow moisture diffusion is strongly affected by the period of the RH fluctuation. When RH fluctuation is slower, the response of the system becomes much more pronounced. In practical terms, this means that a typical oil paint film is much less sensitive to high frequency RH oscillations than to longer timescale weather/seasonal fluctuations. It should be pointed out that the thickness of the test monolayer (500 μm) is approximately 10 times thicker than a typical paint layer. The thickness of the layer strongly affects the water concentration profile as well. In fact, it follows directly from Fick's second law that increasing the thickness has the opposite effect of increasing D. More precisely, decreasing the value of D with factor x is equivalent to increasing the thickness with the square root of x.

The sensitivity study clearly shows that the model is not equally sensitive to each of its input parameters. The isotherm (isotherm shape and c_{95}) has limited impact on the overall response of a

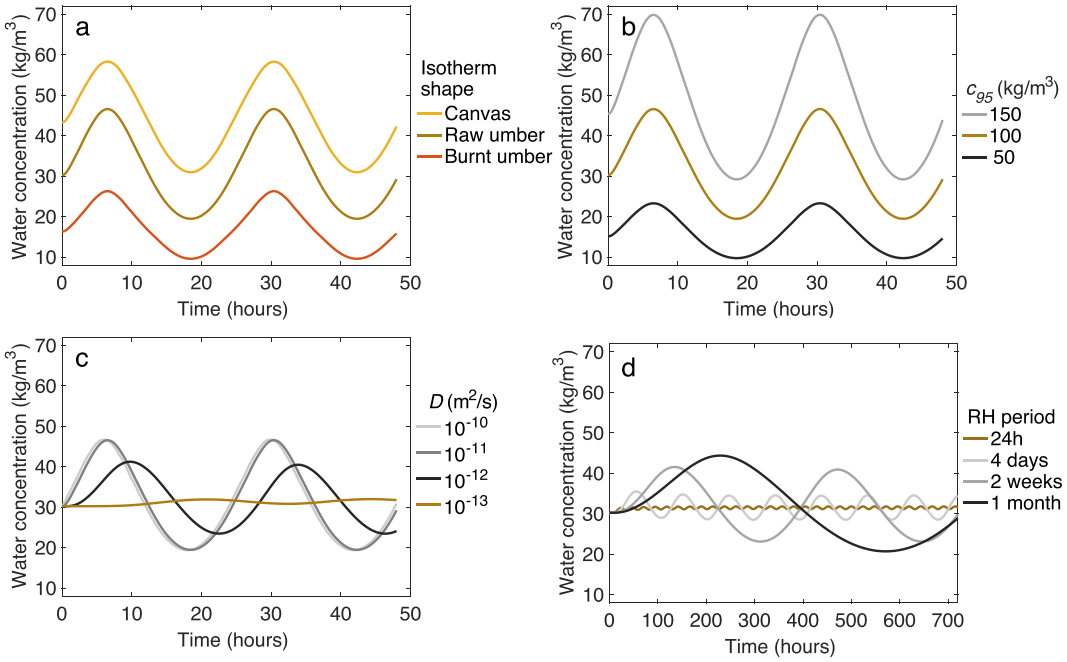

Fig. 8. **a)** Time profile of the water concentration in the centre of the test monolayer with different isotherms. The other parameters were kept constant ($D = 10^{-11}$ m^2/s; $c_{95} = 100$ kg/m^3; thickness = 500 μm, RH period = 24h, $n = 500$). **b)** Time profile of the test monolayer with different c_{95} ($D = 10^{-11}$ m^2/s; thickness = 500 μm; isotherm = raw umber oil paint, RH period = 24h). **c)** Time profile of the test monolayer with different D (thickness = 500 μm; isotherm = raw umber oil paint, $c_{95} = 100$ kg/m^3, RH period = 24h). The brown curve corresponds to the properties of raw umber oil paint. **d)** Time profile of the test monolayer with different RH periods ($D = 10^{-13}$ m^2/s, thickness = 500 μm; isotherm = raw umber oil paint, $c_{95} = 100$ kg/m^3). The brown curve corresponds to the brown curve in (c).

layer to external RH fluctuations, at least within the uncertainty ranges that are relevant to this study. On the other hand, the thickness of a layer, the diffusion coefficient and the period of RH oscillation each have a strong effect on the response. It is important to note that the diffusion coefficient was varied here with entire orders of magnitude, and that smaller variations will have less impact. As a consequence, a rougher estimate of the diffusion coefficient is adequate for modelling the general behaviour of a system. In absolute terms, the model is much more sensitive to variations in layer thickness. In real paintings, however, the thickness of each layer does not vary with orders of magnitude. In short, the moisture response of a multi-layered system will be determined mostly by the combination of D and thickness of the layers, and the RH period. Finally, it is useful to note that the order in which the layers are arranged can have a profound effect on the behaviour of individual layers. A low response layer can act as a barrier to an underlying layer with high response properties and dampen its moisture fluctuations.

3.3. Case study: painted wall hangings in the Hofkeshuis in Almelo

In this section the results of the moisture transport modelling are presented. We used the model to investigate whether a difference in relative humidity between the room and behind the painted wall hangings on the south wall led to gradient in water concentration in the paint layers.

First, the environmental data was further analysed to gain more insight into the environmental conditions in the room and the origin of the difference in RH. The RH behind the canvas on the south wall was found to be on average 7% higher than the air in the room measured close to the west wall (Fig. 9). The air temperature in the room was 22.3 °C on average, while the surface temperature of the reverse was 18.5°C on average. Using these temperatures, the absolute humidity was calculated. The absolute humidity in the room was actually very similar to that behind the canvas at 7.7 and 7.5 kg/m^3, respectively. It is important to note that air temperatures cannot be compared directly to surface temperatures. Nevertheless, these findings indicate that on the south wall the temperature behind the painting is lower than at the front. Therefore, the differences in RH between the front and the back of the painted canvas may be a simple consequence of a temperature difference rather than a gradient in absolute air humidity.

Fig. 10 shows the results of integrating the recorded RH values into the model. This plot is a depth profile, showing the concentration of water in the three layers. The colour in the plot indicates how many days of the year the multilayer experiences a particular water concentration at each depth. A few interesting observations can be made. First, the water concentration in the canvas varies more widely than in the other layers. This variation is probably a consequence of the high moisture diffusion coefficient in canvas, allowing the layer to respond quickly to RH fluctuations. Although the diffusion coefficient in the ground layer is similar, the water concentration in this layer is more stable because its position in the middle of the system shields it from external RH fluctuations. On the left, the ground layer is protected from fluctuations by the low diffusion coefficient in the paint layer, while on the right side is a very thick layer of canvas. We have noted before that increasing the thickness by a factor 10 has the same effect as decreasing the D by a factor 100. Therefore, the layer of canvas protects the ground layer from fluctuations to a similar degree as the paint layer.

In the paint layer, we can observe a clear gradient in water concentration. On average, the water concentration in the surface paint layer (in the centre of the first 10 μm) is 11.2 kg/m^3 and in

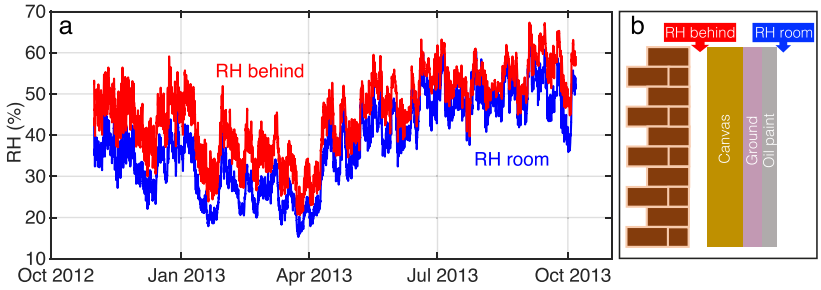

Fig. 9. a) Relative humidity values inside the salon on the first floor of the Hofkeshuis. The blue curve represents the RH of the air in the room, measured close towards the west wall (average value 38.2%). The red curve represents the RH behind the canvas on the south wall (average value: 45.6%). **b)** Schematic representation of the Hofkeshuis case.

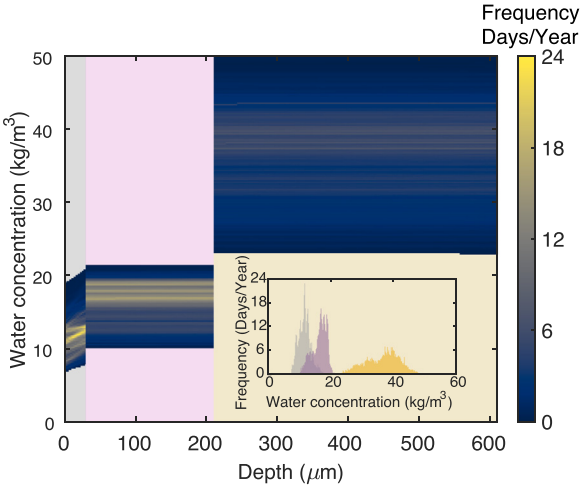

Fig. 10. Depth profile of the layered system representing the painting wall hangings in the Hofkeshuis as a result of the RH data measured in the salon and behind the wall hangings over 334 days. The colour of the curves corresponds to the frequency (days / year). This indicates how many days of the year the materials experience a particular water concentration. The histogram in the insert shows the water concentration distribution in the three layers.

the deeper paint layer (in the centre of the next 20 μm) is 11.9 kg/m^3. This difference is larger when one compares the water concentrations at positions 1 μm and 30 μm ($\Delta c_{\text{paint}} = 1.4$ kg/m^3). A gradient in this direction exists 99% of the year but is not necessarily constant throughout the year as it depends on the RH difference between the front and the back of the painting. Fig. 11a shows that the RH difference is higher in winter than in summer. Fig. 11b shows the water concentration profile in the paint layer on the two days corresponding to the maximum and minimum in ΔRH (20 November and 28 July, respectively). On 28 July, the RH in the room was momentarily higher than behind the canvas. The light blue curve in Fig. 11b corresponds to 80 minutes into this event, when the gradient in water concentration in the paint layer has already changed direction. This result demonstrates that a difference in RH between the front and the back of the painting promptly gives rise to a moisture gradient in the paint layer.

4. Discussion

The case study of the Hofkeshuis presents an example of the type of questions that can be answered using the developed model for moisture diffusion. Our simulations suggest that a difference in relative humidity between the front and the back of the canvas did cause a gradient in water concentration in the paint layers. Moreover, the RH gradient was mostly the result of a difference in temperature rather than a difference in absolute moisture concentration of the air. Technically, this temperature difference violates the assumption of isothermal conditions in the model. Moisture sorption isotherms can shift slightly with changing temperatures. Temperature dependency of sorption isotherms has been studied for coatings (alkyd resin [74], epoxy [75,76]) and several biological materials (corn starch [77], cellulose [78] and flour [79]), revealing a slight shift to higher water concentration with increasing temperature. From Yaseen & Funke, we infer a 0.02–0.13 kg/m^{3}K shift [74]. As our model does not explicitly account for heat transport, the actual temperature difference between the front and the back of the oil paint layers is unknown. However, we can estimate that, to undo the water concentration gradient in the paint layers that we found for the Hofkeshuis case, we would need an unreasonably large temperature difference of 11–70 K between either side of only 30 μm oil paint. Thus, we can safely assume that any isotherm shift will not significantly alter our conclusions.

Our results support the hypothesis that an increased RH behind the painted wall hangings leads to higher water concentrations in the deeper parts of the paint layer compared to the surface. Our simulations show that 99% of the year the paint layer at the surface is dryer than the deeper layer. However, since the absolute values for Δc_{paint} are rather small, it is important to discuss how we should interpret the result of this model. Our aim for this study was to incorporate the existing moisture transport and sorption data into one model to describe the *general* moisture response behaviour of a *generic* oil painting. Of course, there is no such thing as a generic oil painting. Each object is unique, with regards to the time and place in which it was created and its physical and conservation history. We found, however, that each component of a painting has rather distinct sorption and transport properties. The variations in properties for one class of materials encountered in literature were therefore relatively minor compared to the variations between the different components in a painting stratigraphy. It is this diversity in properties that allows us to make useful general predictions.

Fickian diffusion is a basic approximation for moisture transport through an oil painting and it does not consider dimensional change caused by the uptake of water. In zinc and lead-containing linseed oil model systems, minimal swelling due to water uptake has been reported [3]. However, minimal swelling may not be a valid approximation for the other materials found in an oil painting. Clays, for example, which may be present in naturally sourced pigments, can experience expansion due to moisture sorption. Canvas is known to experience some degree of swelling, leading to mechanical stresses [80]. If the dimensional change as a result of varying RH or moisture content is known, it is possible to incorporate layer swelling into the current model following the ap-

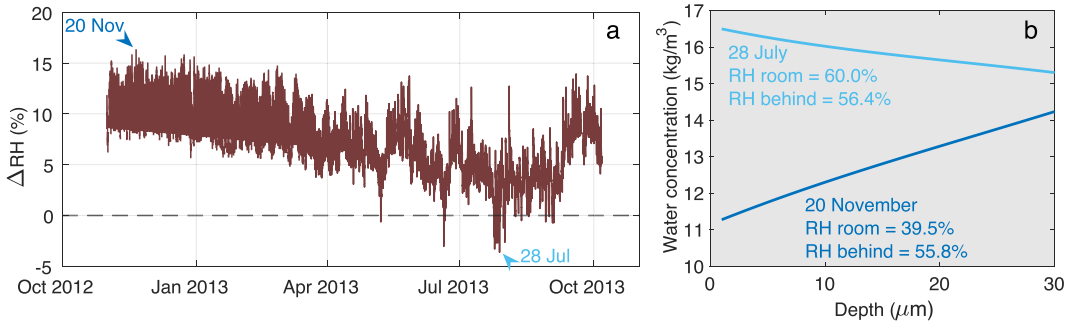

Fig. 11. a) Difference in RH between the front and the back of the painted wall hangings in the Hofkeshuis (RH_{behind} – RH_{room}). The maximum ΔRH is on 20 November 2012 and the minimum on 28 July 2013. **b)** Depth profile in the paint layer of the system representing the painting wall hangings in the Hofkeshuis on 20 November and 28 July.

proach by Baij and co-workers (2018) [3]. In addition, any chemical changes such as dissolution of water-soluble materials are currently not considered.

The current model assumes solid layers with constant thickness. Typical features of heritage objects such as material heterogeneity or craquelure are not reflected by the assumption of homogeneous layers. Cracks could facilitate capillary transport of water, when they are not filled with varnish or other material. Variation in the thickness of the layers is also commonly encountered in paintings like those in the Hofkeshuis case. In some areas in the wall hangings, a thin layer was found between the canvas and the ground containing silicate (earth) pigments bonded with animal glue [65], which was applied to smooth the rough surface of the canvas. Because of this function, this glue layer is not constant in thickness. In addition, no moisture sorption and transport properties of such a layer were known to us. We have chosen here to simplify the stratigraphy and omit this layer, though the effects of such an inhomogeneous intermediate layer could be investigated by constructing a transport model in 2 or 3 dimensions.

Despite the complexity of heritage materials and the intrinsic simplification of any model, we view our model as a useful tool in the (preventive) conservator's toolbox. A modelling approach can provide insights into the moisture response of complicated systems that are very difficult to achieve otherwise. A major strength of the modelling approach is the possibility to quickly analyse multiple scenarios when encountering uncertainties in layer properties or dimensions, and the ability to couple calculations to experimental environmental data. These capabilities will contribute to an intuition for the relative importance of material parameters, as we hope to have demonstrated with the sensitivity study in Section 3.2. Certainly, validating the model against experiments and incorporating more experimental data on moisture sorption and transport properties of heritage materials, especially aged materials, will be important to provide more robust estimates and reliable results. Even with the current limited availability of this data, however, we have contributed to a basic understanding of moisture transport and distribution in a complex, multi-layered system. This work does not yet connect moisture content to chemical deterioration. As such, it is not yet clear whether the calculated gradient in water concentration is sufficient to cause the observed chemical deterioration pattern. The next crucial steps towards developing damage functions for paintings include studying the relations between the (variation in) water concentration and chemical degradation processes. In addition, the current approach could be expanded to include coupled heat and moisture transport and account for temperature effects more accurately. Besides the link between temperature and moisture transport [81], temperature gradients could also influence chemical reaction kinetics inside oil paint layers.

5. Conclusion

In this study, a numerical Fickian diffusion model was developed describing the general moisture response of oil paintings. This model does not only consider paint layers, but the full stratigraphy of the painting, including the support and preparation layers. Based on experimental data available in literature, estimates can be made for the model parameters describing the moisture sorption and transport properties of each component of the painting. The model was applied to the case study of the painted wall hangings in the Hofkeshuis (the Netherlands). Our simulations indicate that a higher relative air humidity behind than in front of the painted canvas leads to a higher concentration of water in the lower paint layer. These results support the hypothesis that an increased relative air humidity behind the painted wall hangings contributed to the observed lead soap deterioration pattern. In general, the case study illustrates the type of conservation-related questions that can be investigated with the presented moisture diffusion transport model, and it shows how our approach generates general insights into the response of a painting to varying environmental conditions.

Declaration of Competing Interest

The authors declare that they have no known competing financial interests or personal relationships that could have appeared to influence the work reported in this paper.

CRediT authorship contribution statement

Jorien R. Duivenvoorden: Conceptualization, Methodology, Investigation, Writing – original draft. **Rick P. Kramer:** Investigation, Writing – review & editing. **Margriet H. van Eikema Hommes:** Investigation, Writing – review & editing. **Piet D. Iedema:** Methodology, Supervision, Writing – review & editing. **Joen J. Hermans:** Conceptualization, Methodology, Supervision, Writing – review & editing. **Katrien Keune:** Conceptualization, Supervision, Writing – review & editing.

Data availability

Data will be made available on request.

Acknowledgements

This research was kindly supported by Bennink Foundation/Rijksmuseum Fonds. JH is supported by The Netherlands Organization for Scientific Research (NWO) under project number 016.Veni.192.052. The investigations in the Hofkeshuis were performed as part of the NWO Incentives Scheme Vidi project From

Isolation to Coherence: an Integrated Technical, Visual and Historical Study of 17th and 18th Century Dutch Painting Ensembles (2012–2018), led by Margriet van Eikema Hommes. The authors would like to thank the residents of the Hofkeshuis for their cooperation during the investigations and the environmental monitoring campaign.

Supplementary materials

Supplementary material associated with this article can be found, in the online version, at doi:10.1016/j.ijheatmasstransfer.2022.123682.

References

[1] S. Cather, Assessing causes and mechanisms of detrimental change, in: R. Gowing, A. Heritage (Eds.), Conserving the Painted Past: Developing Approaches to Wall Painting Conservation, James & James, London, 2003, pp. 64–71.
[2] L. Baij, J.J. Hermans, K. Keune, P.D. Iedema, Time-dependent ATR-FTIR spectroscopic studies on fatty acid diffusion and the formation of metal soaps in oil paint model systems, Angew. Chem. Int. Ed. 57 (2018) 7351–7354, doi:10.1002/anie.201712751.
[3] L. Baij, J.J. Hermans, K. Keune, P.D. Iedema, Time-dependent ATR-FTIR spectroscopic studies on solvent diffusion and film swelling in oil paint model systems, Macromolecules 51 (2018) 7134–7144, doi:10.1021/acs.macromol.8b00890.
[4] L. Baij, L. Chassouant, J.J. Hermans, K. Keune, P.D. Iedema, The concentration and origins of carboxylic acid groups in oil paint, RSC Adv. 9 (2019) 35559–35564, doi:10.1039/c9ra06776k.
[5] M. Beerse, K. Keune, P.D. Iedema, S. Woutersen, J.J. Hermans, The evolution of zinc carboxylate species in oil paint ionomers, ACS Appl. Polym. Mater. 2 (2020) 5674–5685, doi:10.1021/acsapm.0c00979.
[6] A. Burnstock, Taking different forms: Metal soaps in paintings, diagnosis of condition, and issues for treatment, in: F. Casadio, K. Keune, P. Noble, A. van Loon, E. Hendriks, S.A. Centeno, G. Osmond (Eds.), Metal Soaps in Art, Springer, Cham, 2019, pp. 243–262.
[7] F. Casadio, L. Bellot-Gurlet, C. Paris, Factors affecting the reactivity of zinc oxide with different drying oils: a vibrational spectroscopy study, in: F. Casadio, K. Keune, P. Noble, A. van Loon, E. Hendriks, S.A. Centeno, G. Osmond (Eds.), Metal Soaps in Art, Springer, Cham, 2019, pp. 153–172.
[8] J. Catalano, A. Murphy, Y. Yao, N. Zumbulyadis, S.A. Centeno, C. Dybowski, Understanding the dynamics and structure of lead soaps in oil paintings using multinuclear NMR, in: F. Casadio, K. Keune, P. Noble, A. van Loon, E. Hendriks, S.A. Centeno, G. Osmond (Eds.), Metal Soaps in Art, Springer, Cham, 2019, pp. 69–84.
[9] J. Catalano, V. Di Tullio, M. Wagner, N. Zumbulyadis, S.A. Centeno, C. Dybowski, Review of the use of NMR spectroscopy to investigate structure, reactivity, and dynamics of lead soap formation in paintings, Magn. Reson. Chem. 58 (2020) 798–811, doi:10.1002/mrc.5025.
[10] M. Cotte, E. Checroun, J. Susini, P. Dumas, P. Tchoreloff, M. Besnard, P. Walter, Kinetics of oil saponification by lead salts in ancient preparations of pharmaceutical lead plasters and painting lead mediums, Talanta 70 (2006) 1136–1142, doi:10.1016/j.talanta.2006.03.007.
[11] S. Garrappa, E. Kočí, S. Švarcová, P. Bezdička, D. Hradil, Initial stages of metal soaps formation in model paints: the role of humidity, Microchem. J. 156 (2020) 104842, doi:10.1016/j.microc.2020.104842.
[12] V. Gonzalez, A. van Loon, S.W. Price, P. Noble, K. Keune, Synchrotron micro-XRF and micro-XRD-CT reveal newly formed lead–sulfur compounds in old master paintings, J. Anal. At. Spectrom. 35 (2020) 2267–2273, doi:10.1039/d0ja00169d.
[13] C. Grech, N. Tse, A. Doronila, X. Duan, A. Ahmad, M. Mat Isa, A preliminary investigation into the behavior of modern artists' oil paints in a hot and humid climate, in: K.J. van den Berg, I. Bonaduce, A. Burnstock, B. Ormsby, M. Scharff, L. Carlyle, G. Heydenreich, K. Keune (Eds.), Conservation of modern oil paintings, Springer, Cham, 2019, pp. 419–435.
[14] J.J. Hermans, K. Keune, A. van Loon, P.D. Iedema, Toward a complete molecular model for the formation of metal soaps in oil paints, in: F. Casadio, K. Keune, P. Noble, A. van Loon, E. Hendriks, S.A. Centeno, G. Osmond (Eds.), Metal Soaps in Art, Springer, Cham, 2019, pp. 47–67.
[15] J. Hermans, L. Zuidgeest, P.D. Iedema, S. Woutersen, K. Keune, The kinetics of metal soap crystallization in oil polymers, Phys. Chem. Chem. Phys. 23 (2021) 22589–22600, doi:10.1039/d1cp03479k.
[16] K. Keune, J.L. Mass, F. Meirer, C. Pottasch, A. van Loon, A. Hull, J. Church, E. Pouyet, M. Cotte, A. Mehta, Tracking the transformation and transport of arsenic sulfide pigments in paints: synchrotron-based x-ray micro-analyses, J. Anal. At. Spectrom. 30 (2015) 813–827, doi:10.1039/c4ja00424h.
[17] A. van Loon, Color changes and chemical reactivity in seventeenth-century oil paintings, PhD thesis, Universiteit van Amsterdam, Amsterdam, 2008.
[18] G. Osmond, Zinc soaps: an overview of zinc oxide reactivity and consequences of soap formation in oil-based paintings, in: F. Casadio, K. Keune, P. Noble, A. van Loon, E. Hendriks, S.A. Centeno, G. Osmond (Eds.), Metal Soaps in Art, Springer, Cham, 2019, pp. 25–46.
[19] E. Platania, N.L. Streeton, A. Vila, D. Buti, F. Caruso, E. Uggerud, Investigation of mineralization products of lead soaps in a late medieval panel painting, Spectrochim. Acta A Mol. Biomol. Spectrosc. 228 (2020) 117844, doi:10.1016/j.saa.2019.117844.
[20] E. Possenti, C. Colombo, M. Realini, C.L. Song, S.G. Kazarian, Insight into the effects of moisture and layer build-up on the formation of lead soaps using micro-ATR-FTIR spectroscopic imaging of complex painted stratigraphies, Anal. Bioanal. Chem. 413 (2020) 1–3, doi:10.1007/s00216-020-03016-6.
[21] D. Saunders, J. Kirby, The effect of relative humidity on artists' pigments, Natl. Gallery Tech. Bull. 25 (2004) 62–72.
[22] C.S. Tumosa, D. Erhardt, M.F. Mecklenburg, X. Su, Linseed oil paint as ionomer: synthesis and characterization, in: P.B. Vandiver, J.L. Mass, A. Murray (Eds.), Materials Issues in Art and Archaeology VII: Materials Research Society Symposium, Materials Research Society, Warrendale, 2005, pp. 25–31.
[23] D. Erhardt, C.S. Tumosa, M.F. Mecklenburg, Long-term chemical and physical processes in oil paint films, Stud. Conserv. 50 (2005) 143–150, doi:10.1179/sic.2005.50.2.143.
[24] J.J. Hermans, K. Keune, A. van Loon, R.W. Corkery, P.D. Iedema, Ionomer-like structure in mature oil paint binding media, RSC Adv. 6 (2016) 93363–93369, doi:10.1039/c6ra18267d.
[25] Y. Orlova, R.E. Harmon, L.J. Broadbelt, P.D. Iedema, Review of the kinetics and simulations of linseed oil autoxidation, Prog. Org. Coat. 51 (2021) 106041, doi:10.1016/j.porgcoat.2020.106041.
[26] N.C. Schellmann, Animal glues: a review of their key properties relevant to conservation, Stud. Conserv. 52 (2007) 55–66, doi:10.1179/sic.2007.52.Supplement-1.55.
[27] M.D. Shoulders, R.T. Raines, Collagen structure and stability, Annu. Rev. Biochem. 78 (2009) 929–958.
[28] R.J. Gettens, E.W. FitzHugh, R.L. Feller, Calcium carbonate whites, Stud. Conserv. 19 (1974) 157–184.
[29] S. Hackney, G. Hedley, Measurements of the ageing of linen canvas, Stud. Conserv. 26 (1981) 1–14.
[30] M. Preisner, W. Wojtasik, A. Kulma, M. Zuk, J. Szopa, Flax fiber, in: Kirk-Othmer Encyclopedia of Chemical Technology, Wiley & Sons, Hoboken, 2000, pp. 1–32.
[31] V. Baukh, H.P. Huinink, O.C. Adan, S.J. Erich, L.G. van der Ven, NMR imaging of water uptake in multilayer polymeric films: stressing the role of mechanical stress, Macromolecules 43 (2010) 3882–3889, doi:10.1021/ma1001996.
[32] X. Fan, S. Lee, Q. Han, Experimental investigations and model study of moisture behaviors in polymeric materials, Microelectron. Reliab. 49 (2009) 861–871, doi:10.1016/j.microrel.2009.03.006.
[33] G.S. Park, Transport principles—solution, diffusion and permeation in polymer membranes, in: P.M. Bungay, H.K. Lonsdale, M.N. Pinho (Eds.), Synthetic membranes: Science, engineering and applications, Springer, Cham, 1986, pp. 57–107.
[34] N.S. Sangaj, V. Malshe, Permeability of polymers in protective organic coatings, Prog. Org. Coat. 50 (2004) 28–39, doi:10.1016/j.porgcoat.2003.09.015.
[35] W. Sonderegger, M. Glaunsinger, D. Mannes, T. Volkmer, P. Niemz, Investigations into the influence of two different wood coatings on water diffusion determined by means of neutron imaging, Eur. J. Wood Wood Prod. 73 (2015) 793–799, doi:10.1007/s00107-010-0463-5.
[36] B.D. Vogt, C.L. Soles, R.L. Jones, C.-Y. Wang, E.K. Lin, W. Wu, S.K. Satija, D.L. Goldfarb, M. Angelopoulos, Interfacial effects on moisture absorption in thin polymer films, Langmuir 20 (2004) 5285–5290, doi:10.1021/la035830f.
[37] G. van der Wel, O.C. Adan, Moisture in organic coatings—a review, Prog. Org. Coat. 37 (1999) 1–14.
[38] A. van der Zanden, E. Goossens, The measurement of the diffusion coefficient and the sorption isotherm of water in paint films, Chem. Eng. Sci. 58 (2003) 1521–1530, doi:10.1016/S0009-2509(02)00674-7.
[39] K.N. Allahar, B.R. Hinderliter, D. Tallman, G. Bierwagen, Water transport in multilayer organic coatings, ECS Trans. 6 (2008) 41–55, doi:10.1016/j.porgcoat.2007.09.018.
[40] V. Baukh, H.P. Huinink, O.C. Adan, S.J. Erich, L.G. van Der Ven, Predicting water transport in multilayer coatings, Polymer 53 (2012) 3304–3312, doi:10.1016/j.polymer.2012.05.043.
[41] G.L. Graff, R.E. Williford, P.E. Burrows, Mechanisms of vapor permeation through multilayer barrier films: lag time versus equilibrium permeation, J. Appl. Phys. 96 (2004) 1840–1849, doi:10.1063/1.1768610.
[42] D. Jang, Y.-R. Cho, B. Han, Ideal laminate theory for water transport analysis of metal-coated polymer films, Appl. Phys. Lett. 93 (2008) 363, doi:10.1063/1.2996018.
[43] S. Zid, M. Zinet, E. Espuche, Modeling diffusion mass transport in multiphase polymer systems for gas barrier applications: a review, J. Polym. Sci. B. Polym. Phys. 56 (2018) 621–639, doi:10.1002/polb.24574.
[44] R. Hendrickx, E.S. Ferreira, J.J. Boon, G. Desmarais, D. Derome, L. Angelova, D. Mannes, A. Kaestner, H. Huinink, K. Kuijpers, Distribution of moisture in reconstructed oil paintings on canvas during absorption and drying: a neutron radiography and NMR study, Stud. Conserv. 62 (2017) 393–409, doi:10.1080/00393630.2016.1181899.
[45] J.J. Boon, R. Hendrickx, G. Eijkel, I. Cerjak, A. Kaestner, E. Ferreira, Neutron radiography for the study of water uptake in painting canvases and preparation layers, Appl. Phys. A 121 (2015) 837–847, doi:10.1007/s00339-015-9381-z.
[46] A. Bridarolli, M. Odlyha, G. Burca, J.C. Duncan, F.A. Akeroyd, A. Church, L. Bozec, Controlled environment neutron radiography of moisture sorption/desorption in nanocellulose-treated cotton painting canvases, ACS Appl. Polym. Mat. 3 (2021) 777–788, doi:10.1021/acsapm.0c01073.

[47] D. Mannes, S. Sanabria, M. Funk, R. Wimmer, K. Kranitz, P. Niemz, Water vapour diffusion through historically relevant glutin-based wood adhesives with sorption measurements and neutron radiography, Wood Sci. Tech. 48 (2014) 591–609, doi:10.1007/s00226-014-0626-3.
[48] C.K. Andersen, A.A. Freeman, M.N. Mortensen, V. Beltran, M. Łukomski, A. Phenix, Mechanical and moisture sorption properties of commercial artists' oil paint by dynamic mechanical thermal analysis (DMA), nanoindentation, and dynamic vapour sorption (DVS), in: K.J. van den Berg, I. Bonaduce, A. Burnstock, B. Ormsby, M. Scharff, L. Carlyle, G. Heydenreich, K. Keune (Eds.), Conservation of modern oil paintings, Springer, Cham, 2019, pp. 403–418.
[49] T. Chan, M. Odlyha, The effect of relative humidity and pigment type on paint films, Thermochim. Acta 269 (1995) 755–767.
[50] C. Gregers-Høegh, M.N. Mortensen, M.E. Christensen, C.K. Andersen, Distorted oil paintings and wax-resin impregnation–a kinetic study of moisture sorption and tension in canvas, J. Cult. Herit. 40 (2019) 43–48, doi:10.1016/j.culher.2019.05.017.
[51] R. Hendrickx, G. Desmarais, M. Weder, E.S. Ferreira, D. Derome, Moisture uptake and permeability of canvas paintings and their components, J. Cult. Herit. 19 (2016) 445–453, doi:10.1016/j.culher.2015.12.008.
[52] V. di Tullio, N. Zumbulyadis, S. Centeno, J. Catalano, M. Wagner, C. Dybowski, Water diffusion and transport in oil paints as studied by unilateral NMR and ^{1}H high-resolution MAS-NMR spectroscopy, Chem. Phys. Chem. 21 (2020) 113–119, doi:10.1002/cphc.201900858.
[53] L.V. Angelova, B. Ormsby, E. Richardson, Diffusion of water from a range of conservation treatment gels into paint films studied by unilateral NMR: Part I: acrylic emulsion paint, Microchem. J. 124 (2016) 311–320, doi:10.1016/j.microc.2015.09.012.
[54] E. Richardson, E. Woolley, K. Corda, S. Julien-Lees, S. Pinchin, In situ characterisation of readhesion treatments for ceiling paintings using unilateral NMR, Insight: non-Destr, Test. Cond. Mon. 5 (2017) 249–255.
[55] S. Jakieła, Ł. Bratasz, R. Kozłowski, Numerical modelling of moisture movement and related stress field in lime wood subjected to changing climate conditions, Wood Sci. Tech. 42 (2008) 21–37, doi:10.1007/s00226-007-0138-5.
[56] B. Rachwał, Ł. Bratasz, L. Krzemien´, M. Łukomski, R. Kozłowski, Fatigue damage of the gesso layer in panel paintings subjected to changing climate conditions, Strain 48 (2012) 474–481, doi:10.1111/j.1475-1305.2012.00844.x.
[57] B. Rachwał, Ł. Bratasz, M. Łukomski, R. Kozłowski, Response of wood supports in panel paintings subjected to changing climate conditions, Strain 48 (2012) 366–374, doi:10.1111/j.1475-1305.2011.00832.x.
[58] S. Ferrer, G. Campo-Francés, J. Grau-Bové, I. Bautista-Morenilla, A. Nualart-Torroja, RH simulation model for canvas paintings protected by an aluminium backplate and an additional hygroscopic layer, Herit. Sci. 10 (2022) 1–20, doi:10.1186/s40494-022-00741-2.
[59] D.S.-H. Lee, N.-S. Kim, M. Scharff, A.V. Nielsen, M. Mecklenburg, L. Fuster-López, Ł. Bratasz, C.K. Andersen, Numerical modelling of mechanical degradation of canvas paintings under desiccation, Herit. Sci. 10 (2022) 1–13, doi:10.1186/s40494-022-00763-w.
[60] F. Long, L. Thompson, Diffusion of water vapor in polymers, J. Polym. Sci. 15 (1955) 413–426.
[61] R. MacBeth, The moisture sorption of eleven oil paint samples, Master thesis, The Courtauld Institute of Art, London, 1988.
[62] D. Saunders, A methodology for modelling preservation, access and sustainability, Stud. Conserv. 67 (2022) 1–8, doi:10.1080/00393630.2022.2055933.
[63] M. van Eikema Hommes, P. Bakker, A triumph with no battle: the significance of a painted wall hanging (1778) in the Hofkeshuis in Almelo, Oud Holland–J. Art of the Low Countries 129 (2016) 47–118.
[64] Z. Huijbregts, A. van Schijndel, H.L. Schellen, K. Keune, M.E. Hommes, Computational modelling of the impact of solar irradiance on chemical degradation of painted wall hangings in an historic interior, in: Proceedings of the European COMSOL Conference, 17-19 September 2014, Cambridge, UK, University of Technology Eindhoven, Eindhoven, 2014, pp. 1–6.
[65] K. Keune, R.P. Kramer, Z. Huijbregts, H.L. Schellen, M.H. Stappers, M.H. van Eikema Hommes, Pigment degradation in oil paint induced by indoor climate: comparison of visual and computational backscattered electron images, Microsc. Microanal. 22 (2016) 448–457, doi:10.1017/S1431927616000076.
[66] K. Keune, R.P. Kramer, S. Stangier, M.H. van Eikema Hommes, Impact of lead soaps on the formation of age craquelure, in: F. Casadio, K. Keune, P. Noble, A. van Loon, E. Hendriks, S.A. Centeno, G. Osmond (Eds.), Metal Soaps in Art, Springer, Cham, 2019, pp. 107–121.
[67] A.A. Freeman, N. Fujisawa, A. Bridarolli, C. Bertolin, M. Łukomski, Microscale physical and mechanical analyses of distemper paint: a case study of Eidsborg stave church, Norway, Stud. Conserv (2021) 1–14, doi:10.1080/00393630.2021.1925487.
[68] M.F. Mecklenburg, Determining the acceptable ranges of relative humidity and temperature in museums and galleries. Part 1, structural response to relative humidity, Report of the Museum Conservation Institute, the Smithsonian Institution, Washington, D.C, 2007 https://repository.si.edu/bitstream/handle/10088/7056/Mecklenburg-Part1-RH.pdf (accessed 5 May 2022).
[69] P. Atkins, P.W. Atkins, J. de Paula, Atkins' physical chemistry, tenth ed, Oxford university press, Oxford, 2014.
[70] S.A. Altinkaya, O. Topcuoglu, Y. Yurekli, D. Balkose, The influence of binder content on the water transport properties of waterborne acrylic paints, Prog. Org. Coat. 69 (2010) 417–425, doi:10.1016/j.porgcoat.2010.08.005.
[71] L.F. Shampine, M.W. Reichelt, The MATLAB ODE Suite, SISC 18 (1997) 1–22.
[72] L.F. Shampine, M.W. Reichelt, J.A. Kierzenka, Solving Index-1 DAEs in MATLAB and Simulink, SIAM Rev. 41 (1999) 538–552.
[73] C. He, S. Korposh, R. Correia, L. Liu, B.R. Hayes-Gill, S.P. Morgan, Optical fibre sensor for simultaneous temperature and relative humidity measurement: towards absolute humidity evaluation, Sens. Actuators B Chem. 344 (2021) 130154, doi:10.1016/j.snb.2021.130154.
[74] M. Yaseen, W. Funke, Effect of temperature on water absorption and permeation properties of coatings, J. Oil Colour Chem. Assoc. 61 (1978) 284–291.
[75] G. Bouvet, N. Dang, S. Cohendoz, X. Feaugas, S. Mallarino, S. Touzain, Impact of polar groups concentration and free volume on water sorption in model epoxy free films and coatings, Prog. Org. Coat. 96 (2016) 32–41, doi:10.1016/j.porgcoat.2015.12.011.
[76] C.V. Lacombre, G. Bouvet, D. Trinh, S. Mallarino, S. Touzain, Effect of pigment and temperature onto swelling and water uptake during organic coating ageing, Prog. Org. Coat. 124 (2018) 249–255, doi:10.1016/j.porgcoat.2017.11.022.
[77] G. Peng, X. Chen, W. Wu, X. Jiang, Modeling of water sorption isotherm for corn starch, J. Food Eng. 80 (2007) 562–567, doi:10.1016/j.jfoodeng.2006.04.063.
[78] Ç. Meriçer, M. Minelli, M.G. Baschetti, T. Lindström, Water sorption in microfibrillated cellulose (MFC): the effect of temperature and pretreatment, Carbohydr. Polym. 174 (2017) 1201–1212, doi:10.1016/j.carbpol.2017.07.023.
[79] B. Brett, M. Figueroa, A. Sandoval, J. Barreiro, A. Müller, Moisture sorption characteristics of starchy products: oat flour and rice flour, Food Biophys. 4 (2009) 151–157, doi:10.1007/s11483-009-9112-0.
[80] C.L. Andersen, M. Scharff, J. Wadum, M.F. Mecklenburg, With the best intentions: changed response to relative humidity in wax-resin lined early 19th century canvas paintings, in: J. Bridgland (Ed.), ICOM-CC 17th Triennial Conference Preprints, Melbourne, 15–19 September 2014, The International Council of Museums, Paris, 2014 art. 1301.
[81] R. Blahnik, Problems of measuring water sorption in organic coatings and films, and calculations of complicated instances of moistening, Prog. Org. Coat. 11 (1983) 353–392.